Received: 2 July 2023 | Revised: 1 November 2023 | Accepted: 28 November 2023

DOI: 10.1002/inf2.12527

RESEARCH ARTICLE

WILEY

Stretchable spring-sheathed yarn sensor for 3D dynamic body reconstruction assisted by transfer learning

Ronghui Wu[1,2,3] | **Liyun Ma**[1,3] | **Zhiyong Chen**[1] | **Yating Shi**[1] | **Yifang Shi**[1] | **Sai Liu**[4] | **Xiaowei Chen**[1] | **Aniruddha Patil**[1] | **Zaifu Lin**[1] | **Yifan Zhang**[3] | **Chuan Zhang**[5] | **Rui Yu**[1] | **Changyong Wang**[6] | **Jin Zhou**[6] | **Shihui Guo**[1] | **Weidong Yu**[1,3] | **Xiang Yang Liu**[1]

[1]College of Ocean and Earth Sciences, State Key Laboratory of Marine Environmental Science, College of Physical Science and Technology, School of Informatics, Xiamen University, Xiamen, the People's Republic of China

[2]Prizker School of Molecular Engineering, The University of Chicago, Chicago, Illinois, USA

[3]Key Laboratory of Textile Science &Technology, Ministry of Education, College of Textiles, Donghua University, Shanghai, the People's Republic of China

[4]College of Textile Science and Engineering (International Institute of Silk), Zhejiang Sci-Tech University, Hangzhou, the People's Republic of China

[5]Chongqing Academy of Metrology and Quality Inspection, Chongqing, the People's Republic of China

[6]Beijing Institute of Basic Medical Sciences, Beijing, the People's Republic of China

Correspondence
Ronghui Wu, Weidong Yu, and Xiang Yang Liu,
Email: ronghuiwu@uchicago.edu, wdyu@dhu.edu.cn, and liuxy@xmu.edu.cn

Funding information
National Nature Science Foundation of China, Grant/Award Numbers: 62072383, 12074322; Science and Technology Project of Xiamen City, Grant/Award Number: 3502Z20183012; Science and Technology Planning Project of Guangdong Province, Grant/Award Number: 2018B030331001; Shenzhen Science and technology plan project, Grant/Award Number: JCYJ20180504170208402

Abstract

A wearable sensing system that can reconstruct dynamic 3D human body models for virtual cloth fitting is highly important in the era of information and metaverse. However, few research has been conducted regarding conformal sensors for accurately measuring the human body circumferences for dynamic 3D human body reshaping. Here, we develop a stretchable spring-sheathed yarn sensor (SSYS) as a smart ruler, for precisely measuring the circumference of human bodies and long-term tracking the movement for the dynamic 3D body reconstruction. The SSYS has a robust property, high resilience, high stability (>18 000), and ultrafast response (12 ms) to external deformation. It is also washable, wearable, tailorable, and durable for long-time wearing. Moreover, geometric, and mechanical behaviors of the SSYS are systematically investigated both theoretically and experimentally. In addition, a transfer learning algorithm that bridges the discrepancy of real and virtual sensing performance is developed, enabling a small body circumference measurement error of 1.79%, noticeably lower than that of traditional learning algorithm. Furtherly, 3D human bodies that are numerically consistent with the actual bodies are reconstructed. The 3D dynamic human body reconstruction based on the wearing sensing system and transfer learning algorithm enables excellent virtual fitting and shirt customization in a smart and highly efficient manner. This wearable sensing

Ronghui Wu and Liyun Ma contributed equally to this work.

technology shows great potential in human-computer interaction, intelligent fitting, specialized protection, sports activities, and human physiological health tracking.

KEYWORDS

3D body reconstruction, remote personalized clothes customization, transfer learning, wearable sensing system, yarn sensor array

1 | INTRODUCTION

In the era of information and the metaverse, coupled with the rise of e-commerce, and the customers' individual demand in the apparel industry, virtual garment design is crucial not only for clothing customization, but for realization of smart lifestyle.[1] In contrast to the traditional garment design process that requires the paper or calico fabric-based patternmaking process based on the torso model,[2] the virtual garment design is time saving, convenient for customers, and offers a variety of styles and functionalities. Holistic capturing of both human body and movement information is critical to personalized clothing design. However, existing works often focus on either aspect: body shapes only[3] or joint movement only.[4] The conventional method of measuring human body size with a soft ruler is time-consuming and provides only static information, ignoring the continuous human movement.[5] Moreover, state-of-the-art body reconstruction method, such as using range cameras or high-end scanners,[5,6] not only involve heavy expense cost, but also result in poor quality and inconvenience to customers. Furthermore, the data on dynamic dimensions of the human body collected using these methods cannot effectively reflect the requirements of clothing comfort and fit during body movements. For instance, due to multidimensional movements at the joints, a single set of static dimension data cannot fully consider the variations in joint motion caused by individual differences. This can potentially lead to unreasonable clothing designs that are unsuitable for human motion, resulting in discomfort. Therefore, developing a wearable sensing system for human body capture and reconstruction, that is, measure both human body size and track body motion in real time will provide a brand-new idea for clothing customization.

In recent researches, wearable strain sensor[7] shows great potential in human motion tracking[8] and health information detection.[9] Among them, one-dimensional core-shell structured yarn sensors, such as ionotronic silk fibers based sensors,[10] braided yarn sensors,[11] or nanocomposite yarns[12] have demonstrated excellent monitoring performance to the strain. In case of smart yarn sensing rulers that is supposed to monitor the human body dimensions and shape of the garment through the slightest posture-change detection, two requirements are necessary: stable performance throughout the various repeated tests ensured via a feasible processing method and high sensitivity in a low strain range (0%–5%), which are still challenging. Meanwhile, the scalable and simple manufacturing of yarn sensors is immature, particularly because most yarn sensors have complicated structures embedded with conductive nanoparticles or nanowires.[13] Therefore, developing a simplified structured yarn strain sensor[14] that can be used to detect the slightest posture-change and be invisible on the garment is important for dynamic human body reconstruction and advanced clothing customization. In addition, for such 3D dynamic body reconstruction, the huge differences in human body circumferences between individuals are substantial. It is critical to develop a deep learning algorithm to accurately predict the measured values and body shapes. However, it is a non-trivial task to create the virtual representation of humans, given the sensing data in the real world.[15] Although unlimited 3D human model can be synthesized in a variety of shapes and postures, the gap between real and virtual worlds indicates that the model trained in the virtual world is not directly applicable to the real one.[15] In addition, sensors on smart textiles are often subject to challenges of unpredictable deformation and displacement, causing the deviation from their ideal state in the virtual world. Therefore, a new deep learning algorithm to close the gap between the sensing data with the real data and reduce the reconstruction error need be developed urgently.

To address these issues, a wearable sensing system with a highly stretchable spring-sheathed yarn sensor (SSYS) with transfer learning algorithm that facilitates automatic anthropometric parameter modeling for dynamic human body reconstruction was fabricated to fulfill high-end clothing customization (Figure 1). The sensing system is lightweight, portable, privacy protected, and low cost. The SSYS, which have high sensitivity to human circumference and motion detection, are skin-conformal, highly stretchable, and wearable. This enables the smart cloth to have good breathability, flexibility, and wearing comfort. The stability, response speed, durability

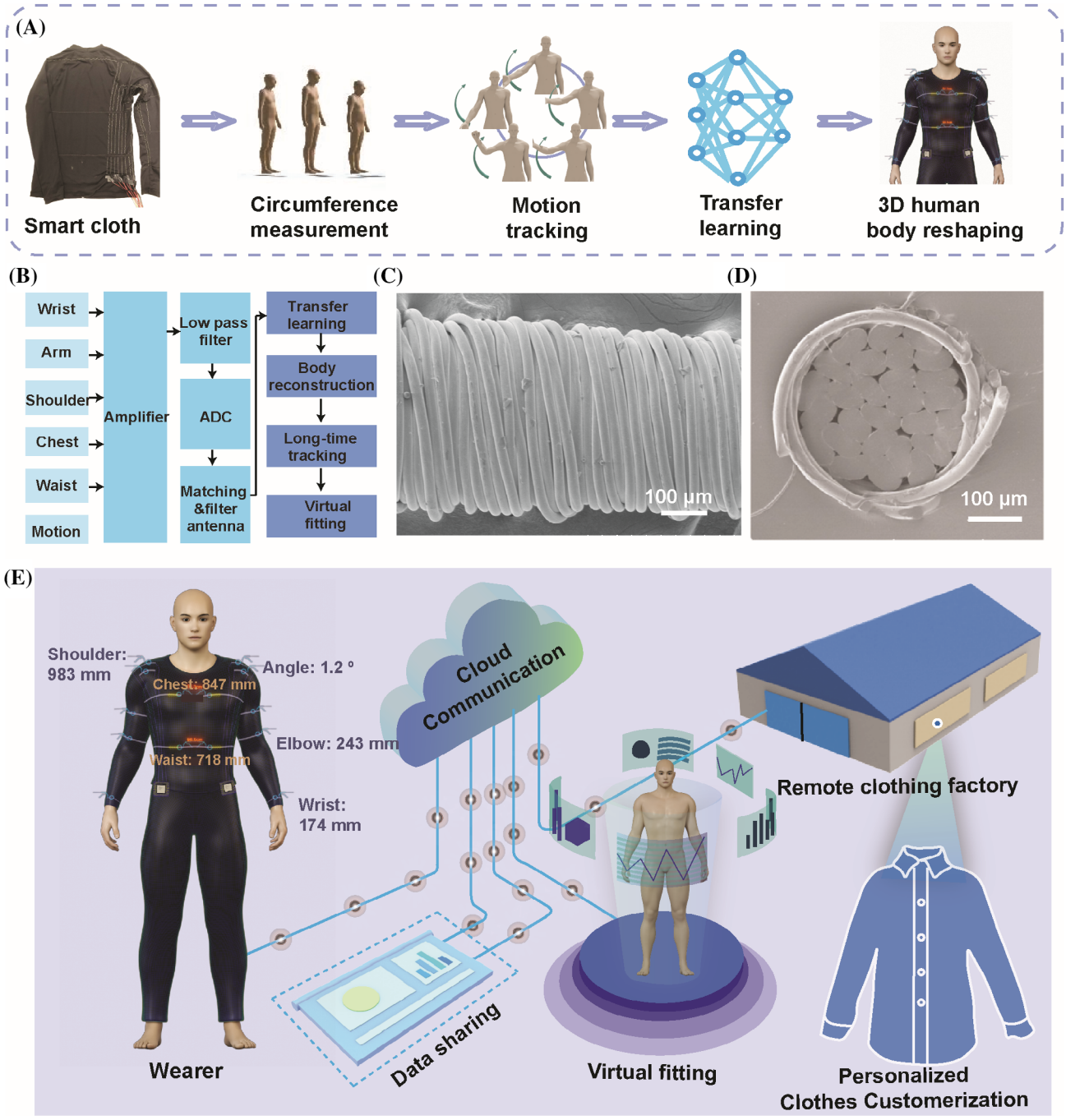

FIGURE 1 Schematic illustration of the wearable sensing system for dynamic human body reconstruction and remote personalized cloth customization. (A) Diagram of the real-time human body reconstruction, showing signal acquisition, data processing, circumferences measurement, motion tracking, and deep learning paths from the SSYS-array-embedded smart cloth to the body reconstruction. (B) Diagram illustration of the wearable multi-channel measuring system. (C,D) SEM images of the longitudinal and cross-sectional view. (E) Remote personalized clothes customization based on the yarn sensing arrays enabled dynamic human body reconstruction.

to external deformation is furtherly studied. Additionally, this sensor can be produced on a large scale with high speed, and it possesses good repeatability and practicality. Moreover, geometric, and mechanical behaviors of the SSYS are systematically investigated both theoretically and experimentally. A transfer learning algorithm is developed to bridge the gap between real and virtual dataset conditions. Furthermore, 3D reconstructed body is reconstructed based on the algorithm. This dynamic human body reconstruction technology combined with transfer learning provide a brand-new method for highly efficient, off-spot, individualized human clothing customization.

2 | RESULTS AND DISCUSSION

2.1 | Wearable sensing system for dynamic human body capture and reshaping

The wearable sensing system for dynamic human body reshaping consists of a SSYS arrays embedded smart cloth and a multi-channel signal collection and processing circuit board (Figure 1A,B). A large dataset is built by measuring the body circumferences by SSYS and fed into the algorithm to train a deep learning model for parameterized human modeling. The connected neural network was used to build a regression mapping from the body circumferences to the corresponding parameters of the human body, while a long short-term memory (LSTM) network was developed to address the challenge of sensor hysteresis and to correct the output electrical signal of the SSYS for accurate posture tracking. By combing the detected human circumferences and motions captured by the wearable sensing system and a large number of samples from the virtual world (Figure S1), transfer learning technology is applied to reconstruct the 3D human models and effectively reduced the error of both shape reconstruction and joint movement tracking.

The facile and low-cost SSYS is fabricated by utilizing the winding and spinning technology, where silver-electroplated polyamide (PA) yarns are used for wrapping and high-elastic spandex yarns are used for supporting (Figure S2). The SSYS has an apparent and uniform core-sheath wrapping structure, with elastic PU fibers as core, and spring-like PA fibers as the sheath, as shown in Figure 1C,D. Meanwhile, because of the high-designated twist of PA wrapping parameter, stacking can be seen between the sheath fibers. Owing to the special wrapping yarn structure design, the SSYS are conformal, highly stretchable, and flexible, enables them to be freely integrated in smart clothes. In this work, to realize the 3D dynamic body reconstruction, SSYS are sewed not only on the wrist, arm, shoulder, chest, and waist of the cloth for human body dimension measurement (Figure 1A), but also on the back of the cloth sleeve as well as around the shoulder to facilitate human joint movement, posture detection, and long-time activity tracking (Figure S1).

The virtual 3D human body reconstructed by wearable sensing system can be furtherly used for the virtual try-on and the customization of shirt. The wearing sensing system is very lightweight with low price and highly efficient, and can protect consumers' privacy and provide them convenience, as shown in Figure 1E.

2.2 | Mechanical property and mathematical models for SSYS sensing unit

To achieve precise data collection and measurement, and improve the automatic parameter modeling for dynamic human body reconstruction, we have studied the SSYS sensing units' deterministic performances from two aspects: mechanical performance and mathematical modeling. In terms of mechanical performance, we focus on developing the stain sensors that can accurately capture and measure specific body movements and dimensions. The strain sensors should be strong and sensitive enough to detect subtle changes in joint angles and body posture. By ensuring the mechanical properties, reliability, and accuracy of the SSYS sensing units, we can enhance the quality of data collection for dynamic body measurements. Here, the static and dynamic mechanical performance of the stain sensors have been systematically studied both experimentally and theoretically. Figure 2A shows the stress–strain curves for SSYS within the strain of 0%–100%. The twist of the SSYS (T_t) determines the spiral status of the sheath filament layer and is controllable through the horizontal movement control motor and winding shaft control motor. It can seen that modulus enhances with the twist increases. The SSYS with twist of 300 has a low Young's modulus of less than 0.7 cN/tex (Figure S3), enabling a soft feature for body conformality. A statistical analysis of the stress amplitudes produced by the sensor during repeated cycles of stretching and relaxation is carried out to predict its fatigue performance in Figure 2B,C. The stress amplitude reduces when the stretching and releasing cycles accumulates, as demonstrated by the typical stress–strain hysteresis loops for 6000 repeating cycles. The bilogarithmic curve for stress–cycle number (S–N) is depicted in Figure 2C. The data show a linear relationship, with a correlation coefficient is 0.968, the S–N curve can be obtained as follows:

$$\log\sigma = -0.0094\log N + 0.946 \quad (1)$$

where σ and N refer to the stress and repeated number, respectively. This characteristic equation represents the basis for yarn sensor lifespan prediction. In real application, the stress loss of SSYS after a certain number of cyclic stretching N can be calculated by invoking the equation.

When the SSYS is stretched, the stress exerted on SSYS is applied for the elongation of core PU yarn and the straightening of the sheath yarns, which is verified by the simulation results via finite element analysis, as can be seen in Figure 2D. From the dynamic mechanical property in Figure 2E, the storage modulus E' decreases rapidly with the temperature

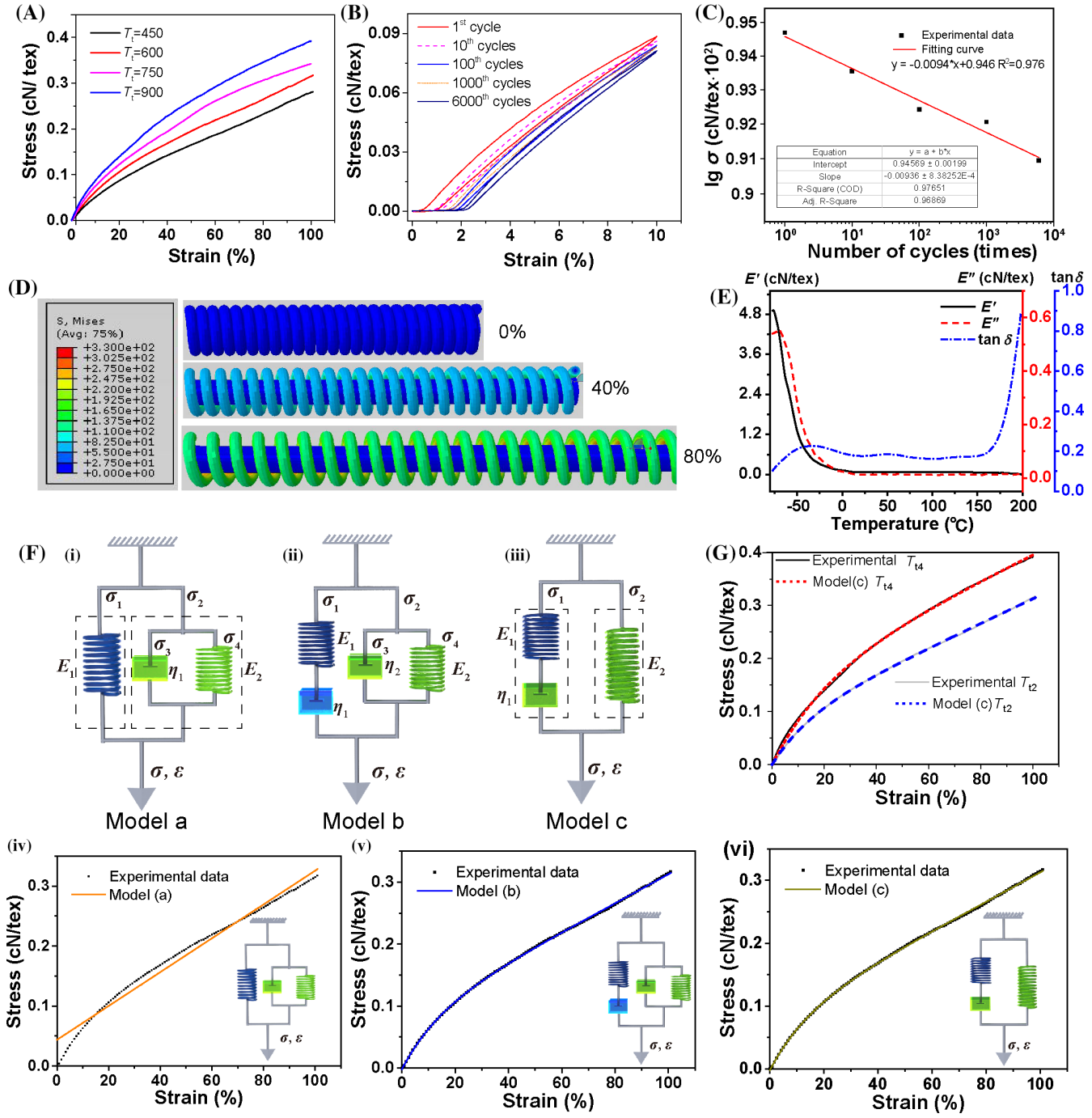

FIGURE 2 Mechanical property and mathematical models for SSYS sensing unit. (A) Stress–strain curves for SSYS with different twists. (B) The elastic hysteresis when SSYS is stretched for the 1st, 10th, 100th, 1000th, and 6000th times. (C) Calculated bilogarithmic stress-cycle number (S–N) curve for the SSYS. (D) Tension distribution when SSYS is stretched into the strain of 0%, 40%, and 80%, predicted by finite element analysis via ABAQUS software. (E) Dynamic mechanical test of SSYS. (F) (i–iii) Three theoretical mechanical models for nonlinear tensile behavior of SSYS. (iv–vi) Comparison between results from three models with experimental data. (G) Comparison of experimental and predicted values of spring sheathed composite yarn with twist of T_{t2} and T_{t4} based on model (c).

increasing from −80°C to 0°C, and the loss of E' reaches to 96%, which is mainly because the glass transition of PU fibers causes the elastic modulus reduction. Meanwhile, the loss modulus E'' of the SSYS shows a slight increase trend in the range of −80°C to −50°C, and then begins to decrease. The loss factor tan δ has two distinct characteristic peaks at −45°C and 60°C, which are caused by the molecular conformational changes in the glass transition region of the PU fibers and the sheath PA filament.

To further clarify the mechanical behavior of SSYS, theoretical rheological models were established based on the core–shell yarn structure. The spring-sheathed SSYS consists of two components, a spandex core yarn parallel to a spring-structured filament shell. Therefore, a Maxwell model of a spring and a viscose Newton dashpot in series were utilized to theoretically simulate the mechanical behavior of the core spandex yarn as well as the interaction with the shell layer, while another spring was used to describe the mechanical performance of the shell layer. Therefore, a three-element model has been established (model a), as shown in Figure 2F(i). The interaction between the sheath layer and core fibers plays a critical role in determining the overall viscoelastic properties of SSYS. To account for this, we incorporate an additional dashpot element, following the principles of model a. Specifically, we introduce a dashpot model in series with the sheath layer yarn's spring to mimic this interaction behavior. Consequently, a four-element model in which the Vigot and Maxwell models are connected in parallel is established, named as theoretical model (b) in Figure 2F(ii). In addition, since the core yarn of the SSYS structure is spandex elastic yarn, its mechanical property tends to be linear in the strain range of 0%–100%, so its viscosity can be ignored. Therefore, we choose a linear spring expression for the core yarn, and the theoretical model (c) is established in Figure 2F(iii). The constitutive equations of the models can be derived as follows:

$$\text{Model a} \quad \sigma = (E_1 + E_2)\varepsilon + k\eta_1 \tag{2}$$

$$\text{Model b} \quad \sigma = k(\eta_1 + \eta_2)\left(1 - e^{-\frac{E_1}{\eta_1}\frac{\varepsilon}{k}}\right) + E_2\varepsilon \tag{3}$$

$$\text{Model c} \quad \sigma = k\eta_1\left(1 - e^{-\frac{E_1}{\eta_1}\frac{\varepsilon}{k}}\right) + E_2\varepsilon \tag{4}$$

where σ is the stress, ε is the strain, E_1 and E_2 are the elastic moduli of the spring, η_1 and η_2 are the viscous coefficients of the Newton dashpot, and k is the strain rate. Figure 2F(iv–vi) shows a comparison of the predicted and measured mechanical curves of the SSYS yarn. The correlation coefficient between the theoretical model (b) and (c) and the measured data are as high as 0.999. Therefore, the four-element model (b) and three-element model (c) that consider the creep effect between sheath and core yarn can simulate the mechanical behavior of the SSYS yarn under stretching. The model (c) is also verified by fitting the experimental data from SSYS with other parameters, as shown in Figure 2G. These mechanical models would provide theoretical guidance for the wearable yarn sensors during stretching.

2.3 | Stretching and bending sensing performance of the SSYS

More importantly, SSYS exhibits excellent sensing performance for subtle strains (0%–5%) during stretching or bending, with significant changes in resistance values. This advantage is of great significance for accurately capturing dynamic data. The sensing mechanism lies in the contact resistance change of the sheath yarn spiral units during stretching. Figure 3A shows the real-time morphologies of the SSYS when it is stretched into 100%. The sheath fibers are separate slowly from originally overlapped status, and such adaption causes the increasement of the SSYS resistance. The twist where the spiral coils of sheath filaments are in contact with each other is assumed to be the critical contact twist (T_{tc}). In this state, the critical sheath pitch (h_c) is equal to the diameter of the sheath filament d_1 (Figure 3B). We can obtain the theoretical critical contact twist as 649 twist/10 cm from the relation, $T_{tc} = 100/d_1$. Accordingly, four twist configurations are designed for the SSYS, that is 450, 600, 750, and 900 twist/10 cm.

When the SSYS has a high twist condition ($T_t > T_{tc}$), the spiral coils partially squeeze and accumulate in the adjacent regions, as shown in the scanning electron microscopy (SEM) image in Figure 3A and the optical images in Figure S3. Based on the structure, the resistance of SSYS would obviously increase during stretching or bending, because the wrapped yarn gradually moves along the stretching direction from the stacked contact state under the action of external force, and the contact between adjacent spiral coils decreases when the pitch h increases (Figure 3C).

Figure 3C shows SSYS has an excellent electrical response to small strains within 40%. The SSYS resistance variation enhanced with the sheath yarn twist increasing from 450 to 750, and the highest gauge factor reach to 65 (Figure 3D). This is because for the SSYS at $T_t < T_{tc}$, the wrapping yarn spiral coils are always in a separated state during stretching, and the contact mode of the spiral coils does not change. Thus, the change in resistance is mainly due to the elongation of the shell filament in the yarn (Figure S6). However, in the initial stretching process, most of the sheath filaments are in the process of spiral coil unwinding with insignificant yarn elongation. When the twist is increased to T_{tc} or above ($T_t > T_{tc}$), the change in resistance of SSYS results from the reduction of the contact area between the sheath yarn bodies and the adjustment of the shortest electron transmission path (Figures S7, S8 and Figure 3A). The resulting rate of change in resistance is therefore the highest. As the twist continues to increase to 900, the contact area between the wrapping filaments continues to become more intensive, allowing the conductive yarn still to be in contact

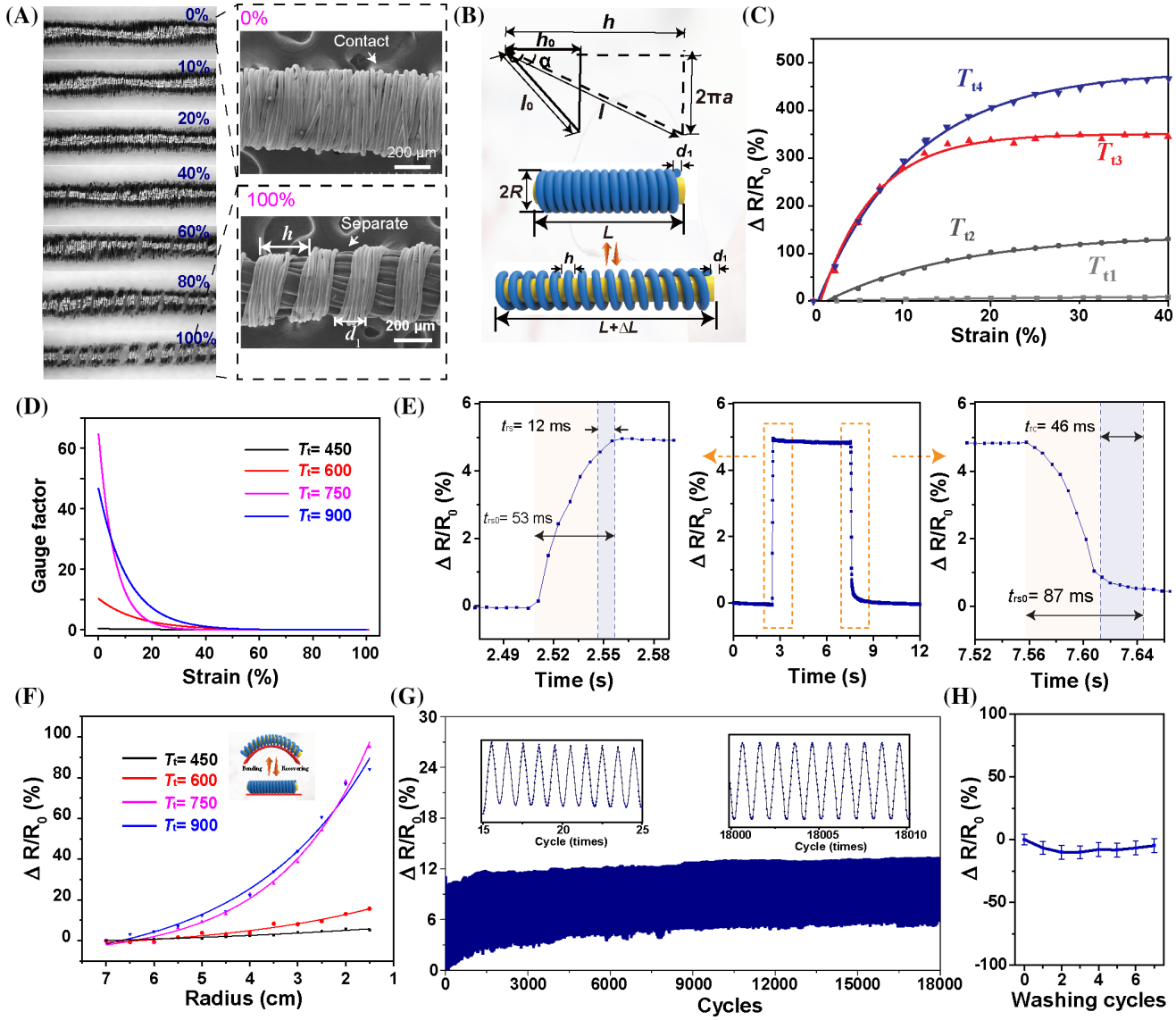

FIGURE 3 Sensing performance of the SSYS. (A) Real-time morphology of SSYS before and after stretching. (B) Schematic of unfolding of the spiral sheath yarn. (C) Relative change in resistance ($\Delta R/R_0$) of SSYS while stretching. (D) Gauge factor of SSYS during stretching. (E) Response (t_{rs}) and recovery time (t_{rc}) of the SSYS when stretched to 1% strain, and kept for 5 s. (F) Relative change in resistance of SSYS when bended into different radius of 7 to 1 cm. (G) Cyclic performance of SSYS during 18 000 times repeated stretching and recovery; insets are the amplification of the signals near the test beginning (15–25th cycle) and the end of the test (18 000–18 010th cycle). (H) Resistance variation of SSYS after 6 times continuous washing test.

with each other within the initial tensile strain. Therefore, it shows a higher resistance changing rate at strain of 40%, but a relative lower gauge factor than 750 twists at the initial strain region. These results can be also concluded from Figure S9 that shows the fitting curves of the strain and resistance change rate in the strain range of 0%–5% for SSYS. The slope of the fitted curve shows that SSYS with twist of 750 has a highest sensitivity, which is consistent with the theoretical calculation of the critical twist. Therefore, we chose to wrap the SSYS with a design parameter of 750 around the clothing to measure the body circumferences as well as for 3D human body reconstruction.

Figure 3E shows a response time of 12 ms (t_{rs}) while loading a 1% strain to the SSYS. Here, the t_{rs} is defined as $t_{rs} = t_{rs0} - t_0$, where t_{rs0} means the measured response time and t_0 is the time needed for strain loading.[16] After 5 s holding, the sensor signal is recovered to the original value once the stress is released, with a short recovery time of 46 ms. Figure 3F shows the high resistance changes when SSYS are bended into different radius. It demonstrates that the SSYS is not only sensitive to the stretching, but also to the bending, which is more frequently happened for the wearable clothes than stretching. Figure 3G shows the high cyclability of SSYS

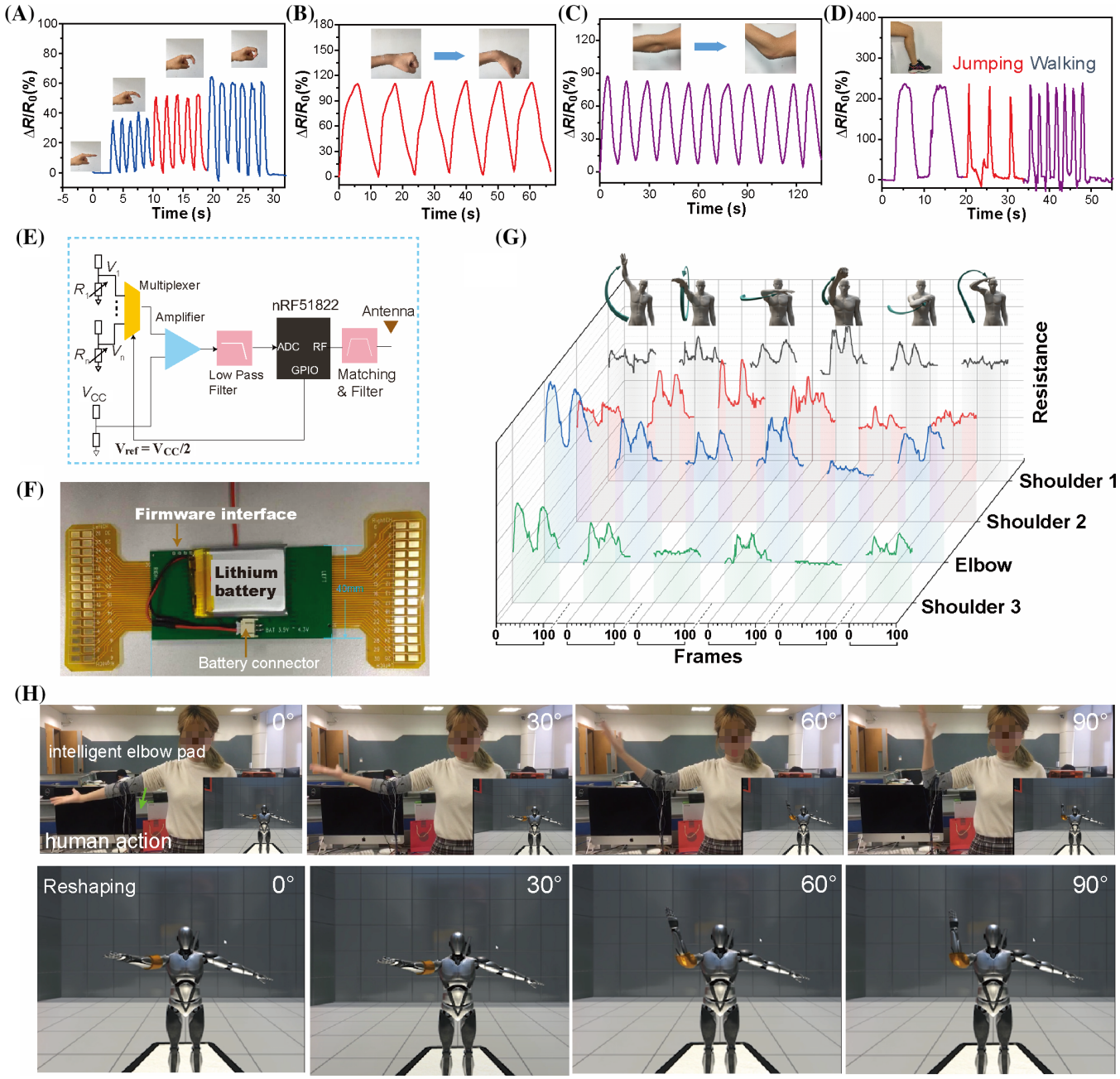

FIGURE 4 SSYS for long-time movement tracking and 3D dynamic human body reconstruction. (A–D) SSYS for human body movement monitoring for (A) finger joint, (B) wrist, (C) elbow, and (D) leg joint. (E) Schematic of the customized circuit board for multi-channel data acquisition and processing. (F) Image of the flexible circuit board. (G) Long-time tracking of various human motions, including raising hand, whirling, waving, fisting, chest pounding, and saluting. (H) Human motion reconstruction.

at 18 000 repetitions of stretching and recovery. The SSYS still exhibit a stable sensitivity at the 18 000th cycle, as shown in the inset of Figure 3G. Moreover, the washability of SSYS is further demonstrated in Figure 3H since it is indispensable for wearing clothes. The resistance didn't change obviously after 6 times washing with detergents. In addition, the SSYS is uniform in length, which can be seen from the similar slope values for the SSYS resistance with different length in Figure S10. The fitting curves and correlation coefficients also demonstrate a linear response within the strain range of 5% for the SSYS. Compared with the reported core-sheath structured yarn sensors,[12,17] SSYS has excellent sensitivity within small deformation range (0%–5%), noticeable cyclability, fast response time, and pronounced washing stability (Table S1).

2.4 | Human body movement detection and long-time tracking using SSYS

To demonstrate the human body movement detection ability, SSYS was attached to various joint parts of human body, such as finger, wrist, elbow, and leg joints. Tiny movement of these joints can be distinguished and detected using SSYS, as shown in Figure 4A–D. The real-time output electrical signal of SSYS is translated into two types of information: human body movement and shape circumferences (Figure S1). Therefore, the visual model of the human body can be further reconstructed for people who wear smart clothes. Here, a customized circuit board was developed to measure the ruler resistance values and transmit them to the server for further processing (Figure 4E) via Bluetooth Low Energy (BLE) using an integrated circuit chip. As shown from the image in Figure 4F, the circuit is composed of a central component and two connection accessories. The central component contains the core electronics for signal reading, processing, and transmitting, while the connection accessory is used for soldering the cables connected with the sensor and the main component. The connection circuit is fabricated with flexible printed circuit. The detachment of the main circuit with the connection accessories offers the flexibility of soldering and maintaining. The two ends of 30 channels are arranged at the two sides of the circuit. The circuit is powered by a Lithium battery, with the capacity of 600 mAh, located at the back of the circuit. The Wheatstone bridge was used to obtain the SSYS resistances from the monitored voltage. Each SSYS is connected to a divider resistor whose resistance value is predetermined from the measured characteristics of the channel. The divider resistor and the SSYS share the standard voltage V_{cc} (3.3 V); therefore, the resistance value of our sensor can be measured by monitoring the voltage (V_i, $i = 1, \ldots n$) at the two ends of the SSYS. In this strategy, we compare the voltage of the SSYS with the reference voltage ($V_{ref} = V_{cc}/2$) and use the difference between the two to measure the change in sensor resistance. This strategy can significantly improve the sensitivity of SSYS resistance measurement.

Using the electrical board, typical electric outputs for various human motions, including raising hand, whirling, waving, fisting, chest pounding, and saluting are detected by four channel sensors, as shown in Figure 4G. These signals can be furtherly processed for dynamic body construction. Figure 4H shows the real-time image and the reconstructed human body when the user wears the SSYS embedded smart elbow. The motion can be real-time reconstructed without obvious delay, as can be seen from Video S1.

2.5 | Smart cloth and machine learning based dynamic 3D reconstruction and cloth customization

Dynamic 3D human body reconstruction is critical for clothes customization not only because it can provide virtual fitting for reconstructed 3D body models, but also it enables personalized size enlargement for cloth design. For example, a person who is more likely to engage in heavy dynamic movements through his/her daily routines would require a more loose-fitting garment. However, the traditional methods to determine the amount of size enlargement is determined subjectively, without considering the customer moving habits. Long-term dynamic tracking will enable a more personalized size enlargement determination for precise clothes customization.

To realize a smart cloth for body circumferences and motion measurement, a smart cloth with 9 SSYS sensors is developed, as shown in Figure 5A. Five SSYS sensors horizontally sewed on chest, waist, shoulder, elbow, and wrist parts are for circumferences measurement of the upper human body. The other four sensors sewed on shoulder and elbow parts are for human motion long-time tracking. To increase the measurement accuracy of SSYS and establish precise 3D models for clothing customization (Figure 5B), a deep learning method was applied, which includes data collection in real (target) domain, data collection in virtual (source) domain, model training in the virtual (source) domain, and transfer learning in the real (target) domain. First, data collection in real world, that is, the real (target) domain, was achieved with the proposed smart clothing system. To prepare the label of body modeling, we measured the body circumferences of 25 subjects (training: 19, testing: 6) with a traditional ruler. To handle the problem of dynamic breathing, we collected the data for five different scenarios, including standard, maximum/minimum belly breathing, maximum/minimum chest breathing. The dataset by interpolating the resistance values and body circumferences between the range of sensing values were further augmented. The interpolation is conducted following the sensor characteristic length-resistance curve (Figure 3C). For the task of motion tracking, a ZED stereo camera was also applied to track human posture to prepare the labeled samples. To furtherly build the synthetic data in the virtual (source) domain, we first used the SMPL[18] method to generate a large archive of 3D human models of different body shapes and postures by setting different values of the shape variable β and the posture variable θ. Each model was represented as a triangular mesh. The virtual sensor is manually marked as the geodesic curve connecting two triangular vertexes on the 3D model. The SSYS-embedded smart cloth was used to measure the body

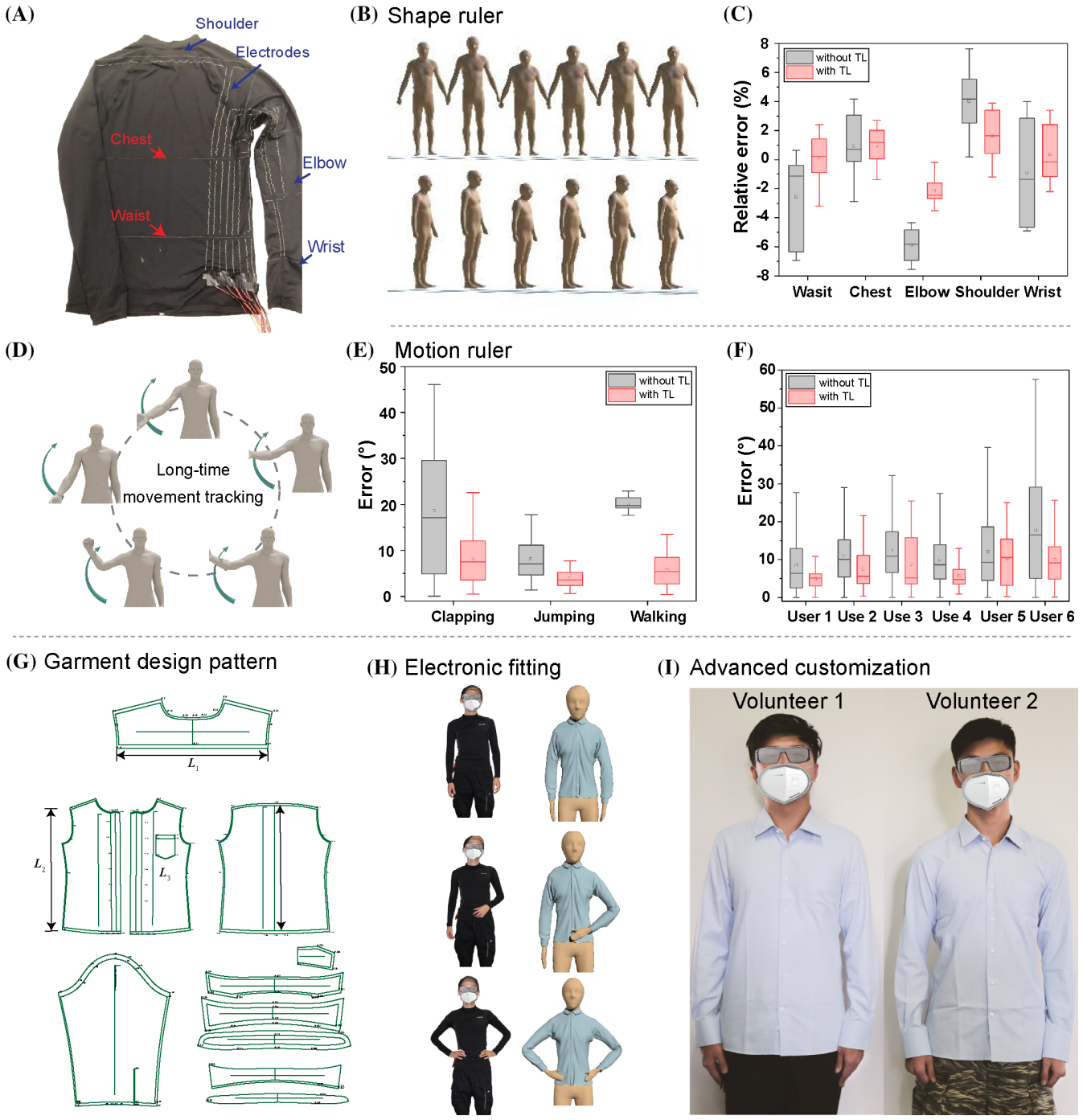

FIGURE 5 Dynamic human body 3D model reconstruction and cloth customization. (A) Image of the SSYS embedded smart garment for human body dimension and action measurement. (B) Six reconstructed human bodies based on the dimension measured by wearing the smart garment shown in (A). (C) Measurement error of body circumference with and without transfer learning (TL) model. The measurement with transfer learning algorithm obviously decreases the measurement errors. (D) Schematic of the long-time tracking and dynamic body movement reconstruction. Measurement error for motion tracking with and without transfer learning for (E) different motion types and six different users. TL evidently diminish the motion measurement errors. (G) Garment pattern design based on the 3D constructed user model. (H) Virtual fitting effect with respect to the volunteer wearing the smart garment. (I) The actual shirt fitting effect for two different volunteers.

circumferences of specific body parts. The ruler placement was determined following the standard 3D Measurement protocol published by the International Organization for Standardization.[19] The body circumferences on the 3D model are equivalent to the circumference of the intersection circle between the

cutting plane and the 3D model. The stretching length of the virtual sensor is the length of the geodesic curve on the 3D model given different human posture. All motion data are randomly divided into the training and testing datasets with the ratio of 8:2.

Furthermore, two neural networks were utilized to predict the human shape and motion in the virtual domain. The mapping between the SSYS length and body shapes was constructed with a fully-connected network (FCN). Motion tracking suffers from the severe problems of sensor hysteresis, deformation, and displacement. To address this problem, the LSTM network was used to translate the sensor values to the predicted posture. The input to the network is the sensor value, while the output is the predicted joint angles (Figure S15). The predicted output of the network was designed to minimize its deviation from the measured sensor length. The loss function was defined as the squared sum of the two. Figure S14 shows the values of the loss functions while training the network model for posture prediction. The result shows the metric on both the training and testing datasets. This confirms the convergence of the network performance on the testing dataset.

Sensor deformation and displacement implies the condition that the sensor undergoes complex deformation, and deviates from its ideal position to track the corresponding joint angle. This is a common issue when using garment-based textile sensors over a long period. This scenario is completely different from the virtual one, where all measures can be accurately computed. To bridge the discrepancy between the real and virtual domains, the technique of transfer learning, DAN[20] was used to build the mapping of data distributions from the source (virtual world) to the target (real world) domains. DAN takes the trained model in the virtual world and the sensing data collected in both virtual and real worlds. Therefore, an FCN model after transfer learning builds a regression mapping from the body circumferences (measured by the SSYS, Figure 5C) to the parameterized human body. The circumferences of six volunteers with different body shapes who had worn the SSYS-embedded SC are used as the testing samples (Figure 5B). The results show that with transfer learning, the average relative measuring error has been obviously reduced from 3.71% to 1.79% (Figure 5C and Table S2). Therefore, there is a high consistency between the manually measured body circumferences and the corresponding predicted values from our SSYS smart garment testing system. Further, the reconstructed human bodies have very similar figures as volunteers, so that they can be further used for virtual clothing fitting, as shown in Figure 5B. We also deployed an LSTM network to address the challenge of sensor hysteresis and correct the output electrical signal of the SSYS for accurate posture tracking. When the volunteers bend the arms in different angles (Figure 5D), the reconstructed human body angles measured by SSYS are consistent with the camera measured values. The error analysis of the measured values and the reconstructed values from the different volunteers are shown in Figure 5E. Obviously, the measurement error by SSYS has been shortened compared to traditional deep learning method. The measurement accuracy based on transfer learning is furtherly proved by the six users' motion reconstruction, as shown in Figure 5F. These results showed that the transfer learning effectively generalizes the trained model in the virtual world to the real one and improves the prediction accuracy in the real world.

Based on the measured circumferences by SSYS and the virtual try-on with the reconstructed body shape, personalized shirt for two volunteers are furtherly demonstrated. To realize that, shirt patterns were explicitly designed based on SSYS measured body circumferences (Figure 5G,H). Accordingly, two tailored shirts that are based on the sensor monitored body sizes show a good fitting on two different volunteers (Figure 5I and Figure S16), demonstrating the advanced clothing customization. Unlike the conventional advanced cloth customization, the dynamic human body reconstruction based human clothing customization system would be of great convenience for customers because of the remote monitoring and fitting functions. As shown in Figure 1E, while someone wears the intelligent garment, the apparent size and motion signals of the body could be detected in real-time. By using a multichannel data collecting method, real-time voltage data of every SSYS unit can be measured simultaneously. Following signal processing and transfer learning, the human body information and the long-time tracked signals will be analyzed and shared in the cloud server; therefore, the cloth designer obtains the real-time human size and motion habit, which plays a guiding role in determining the cloth ease allowance. The cloth factory can design the personal customized clothes according to the information, and consumers can not only witness the cloth fitting effect on the resemble virtual model, but fulfill the cloth advanced customization remotely, even at home. This facile low-cost method facilitates advanced clothing customization and provides a new concept of smart shopping. When customers wear the smart cloth, personal data can be recorded in the cloud database and factory can accordingly fulfill the advanced clothing customization remotely.

3 | CONCLUSION

A wearable sensing system based on yarn stretchable sensor arrays and transfer learning is developed to

reconstruct 3D dynamic human body for garment customization. The full-fiber stretchable sensor SSYS with a high sensitivity in the strain range of 5% is used as a smart ruler for precisely measuring the circumference of human bodies and long-term tracking the movement. The SSYS is mechanically robust, highly stable (>18 000), washable, ultrafast responsive (12 ms) to external deformation, and durable for long-time wearing. A three-element viscoelasticity model which considered the mechanical property of each yarn component is stablished and shows a high correlation coefficient with the experimental data, providing theoretical analysis for the yarn strain sensors. In addition, a smart cloth is designed for human body circumference measurement and long-time movement tracking. With transfer learning algorithm, body circumference measurement error is as low as 1.79%, much lower than that uses traditional learning algorithm. The six virtual bodies reconstructed by this facile method are consistent with the actual human bodies. Well-fitting customized shirt based on the digital SSYS ruler measurement is designed and demonstrated. This dynamic human body reconstruction technology combined with transfer learning provide a brand-new method for highly efficient, off-spot, individualized human clothing customization. This technology has great potential in areas such as human-computer interaction, intelligent fitting, clothing customization, specialized protection, sports activities, and human physiological health.

4 | EXPERIMENTAL SECTION

4.1 | Preparation of smart cloth

The SSYS was fabricated by vertically wrapping a silver-plated polyamide filament on the surface of the PU fiber using a homemade wrapping machine that combines two mechanically rotating agitators allowing the core supporting yarn to rotate at different speeds. The two ends of the pretreated supporting yarn were stabilized in two mechanical agitators, and the silver-plated PA was stabilized with the yarns at one end. The rotating agitators were rotated at speeds of 300–600 rpm, to control the twist of the wrapped yarn; the sheath filaments were wrapped vertically along the core yarn that were controlled by the parallel moving lateral screw. Additional conductive yarns acting as electrodes were constructed on both sides of the composite yarn using a conductive silver paste (DuPont 4929 N) to stabilize the linkage segment. We sewed three SSYS horizontally around the shoulder, chest, and waist of the tight-clothing and two SSYS on the wrist and arm of the right cloth sleeve. Another SSYS was distributed vertically along the back of the sleeve for motion monitoring. Three SSYS were sewed on the shoulder to monitor the body movements. The SSYS and electrodes do not cross each other.

4.2 | Characterization of SSYS morphology and performance

The electrical conductivity of the conductive yarn electrodes and SSYS were measured by a Keithley 2450 source meter at a 1 V AC signal. The surface morphologies were examined using a 710 field-emission scanning electron microscope (FE-SEM). The mechanical performance was evaluated using a microforce testing system (Instron 5948).

4.3 | Signal acquisition and processing

A customized circuit board to measure the sensor resistance values, which are transmitted to the server for further processing. The data were transmitted to the server via Bluetooth Low Energy (BLE) using an integrated circuit chip (Nordic nRF51822). The circuit was composed of 30 channels. The value of each channel was encoded with 10 bits, with a value in the range of 0 to 1023. To increase the efficiency of data processing in the following stages, we used 12 bits (multiples of 4) for each channel and set the first two bits as 0. The sample packet is defined as the data collected from all the channels after a complete sensor reading cycle. In total we had 360 bits (=45 bytes) for each sample packet because the maximum package size for BLE technology is 20 bytes. The complete data for the 25 channels were divided into three packages; a counter byte was added at the end of each package. This counter indicates the number of data transmissions since the system startup and its value is the same across three packages of the same sample packet. This further verifies whether the three data packages are sent and received consistently at the server end.

4.4 | 3D human body reshaping and movement tracking

A regression model, that is, FCN with a correspondence between the body circumferences and the shape variable β in the Skinned Multi-Person Linear (SMPL) model is firstly built.[18] Each model was represented as a triangular mesh. The dataset includes 4400 humanoid models with different shapes. The FCN network was composed of two layers, each of 256 units. Then, the FCN was trained

using the Adam Optimizer with a learning rate of 0.005 and a batch size of 128. The sensor placement for body shape measurement was determined following the standard 3D measurement protocol published by the International Organization for Standardization. After the process of data augmentation, 2500 paired samples of body circumferences and sensor resistance values were produced. The model trained in the virtual domain and the dataset in the real world are fed into the module of Domain Adaptation Network (DAN). This procedure generalizes the model trained in the virtual domain and reduces the prediction error in the real domain.

After reconstructing the body shape, the dataset of different postures is generated in the virtual domain by setting different values of θ in the SMPL model. The dataset includes 2035 motion sequences and 70 733 postures (i.e., 3D humanoid models). The geodesic length of the virtual sensor curve was measured on the 3D model. This serves as the functionality of virtual sensing. Then the LSTM model was used to build the mapping from the virtual sensor length to the posture parameter θ. The LSTM network is composed of three hidden layers, each with 128 hidden units. To train the network, the Adam Optimizer with a learning rate of 0.0025 and a batch size of 64 were used. Six participants wear the garment and conducted routine office activities, including walking, typing on a computer, attending meetings, writing notes, and so on. The sensor signals transmitted via Bluetooth are recorded together with a stereo camera ZED. The posture was estimated with an open-source project, OpenPose.[21] In total, a dataset of approximately 20 000 samples is established, of which 80%, 10%, and 10% were used as the training, validation, and testing datasets, respectively. The data collected in the real world is used for transfer learning with the technique of DAN.

4.5 | Personalized cloth design

After training the model, six participants wore the cloth and conducted their daily activities in an office environment. The garment automatically recorded the resistance values and sent them to the mobile phone; the data were then forwarded the data to the server. The resistance values were mapped to human postures using the aforementioned trained network. Therefore, we obtained the distribution of posture for a specific person in an office environment. This information is used to create a customized cloth at a later stage.

The cloth pattern was obtained from a professional cloth designer. On the design pattern, the positions that corresponded to the measured body circumferences are explicitly marked.

4.6 | Informed Consent

The participants agreed to all tests in the manuscript with informed consent, including the human body reconstruction and cloth fitting tests. The wearable sensors were sewn on the surface of a long-sleeve sport shirt, the sensors do not directly contact the skin of participants. The six participants are all students and faculties at Xiamen University. The participants all understood that the action of measuring circumferences and motion tracking presents no risk of harm. The study conforms to recognized standards.

AUTHOR CONTRIBUTIONS

Ronghui Wu, Liyun Ma, Zhiyong Chen, Shihui Guo, Weidong Yu, and Xiang Yang Liu conceived the work. Ronghui Wu, Liyun Ma, Aniruddha Patil, Yating Shi, Yifang Shi, and Sai Liu designed and fabricated SSYS. Ronghui Wu, Liyun Ma, Sai Liu, Zaifu Lin, Yifan Zhang, Chuan Zhang, Rui Yu, Changyong Wang, and Jin Zhou conducted performance characterization. Zhiyong Chen, Xiaowei Chen, Shihui Guo developed the deep learning algorithm, and conducted experiment of human model reshaping as well as advanced clothing customization. Ronghui Wu, Liyun Ma, Shihui Guo, Weidong Yu, and Xiang Yang Liu wrote the paper with the help of all the authors. Weidong Yu and Xiang Yang Liu supervised the project, assisted in designing the experiments, evaluating the data.

ACKNOWLEDGMENTS

We gratefully acknowledge the National Nature Science Foundation of China (No. 12074322, No. 62072383), Science and Technology Project of Xiamen City (3502Z20183012), Science and Technology Planning Project of Guangdong Province (2018B030331001), Shenzhen Science and technology plan project (JCYJ20180504170208402). The authors thank the technical support received from Shengshi Guo, Yang Yun, Hao Wang, and Likun Yang.

CONFLICT OF INTEREST STATEMENT

The authors declare no conflict of interest.

ORCID

Ronghui Wu https://orcid.org/0000-0002-0752-9383

REFERENCES

1. Tao X, Bruniaux P. Toward advanced three-dimensional modeling of garment prototype from draping technique. *Int J Clothing Sci Technol*. 2013;25(4):266-283.
2. Liu K, Zhu C, Tao X, Bruniaux P, Zeng X. Parametric design of garment pattern based on body dimensions. *Int J Ind Ergon*. 2019;72:212-221.

3. Yunchu Y, Weiyuan Z. Prototype garment pattern flattening based on individual 3D virtual dummy. *Int J Clothing Sci Technol*. 2007;19(5):334-348.
4. Lorussi F, Rocchia W, Scilingo EP, Tognetti A, De Rossi D. Wearable, redundant fabric-based sensor arrays for reconstruction of body segment posture. *IEEE Sens J*. 2004;4(6):807-818.
5. Liu Z, He Q, Zou F, Ding Y, Xu B. Apparel ease distribution analysis using three-dimensional motion capture. *Text Res J*. 2019;89(19-20):4323-4335.
6. (a) Zeng Y, Fu J, Chao H. 3D human body reshaping with anthropometric modeling. *International Conference on Internet Multimedia Computing and Service*. Springer Singapore, Singapore. 2017;819:96-107. (b) Thomassey S, Bruniaux P. A template of ease allowance for garments based on a 3D reverse methodology. *Int J Ind Ergon*. 2013;43(5):406-416.
7. (a) Wang C, Li X, Gao E, et al. Carbonized silk fabric for ultrastretchable, highly sensitive, and wearable strain sensors. *Adv Mater*. 2016;28(31):6640. (b) Liu ZF, Fang S, Moura FA, et al. Hierarchically buckled sheath-core fibers for superelastic electronics, sensors, and muscles. *Science*. 2015;349(6246):400. (c) Hou C, Xu Z, Qiu W, et al. A biodegradable and stretchable protein-based sensor as artificial electronic skin for human motion detection. *Small*. 2019;15(11):1805084. (d) Wang Q, Jian MQ, Wang CY, Zhang YY. Carbonized silk nanofiber membrane for transparent and sensitive electronic skin. *Adv Funct Mater*. 2017;27(9):1605657. (e) Lu Y, Yue Y, Ding Q, et al. Environment-tolerant ionic hydrogel–elastomer hybrids with robust interfaces, high transparence, and biocompatibility for a mechanical–thermal multimode sensor. *InfoMat*. 2023;5(4):e12409. (f) Xiong P, Mengmeng L, Linxuan L, et al. Wearable textile-based in-plane microsupercapacitors. *Adv Energy Mater*. 2016;6(24):1601254. (g) Wang K, Xu W, Zhang W, et al. Bioinspired water-driven electricity generators: from fundamental mechanisms to practical applications. *Nano Res Energy*. 2023;2(1):e9120042.
8. (a) Hammock ML, Chortos A, Tee BC-K, et al. The evolution of electronic skin (e-skin): a brief history, design considerations, and recent progress. *Adv Mater*. 2013;25(42):5997. (b) Wang M, Yan Z, Wang T, et al. Gesture recognition using a bioinspired learning architecture that integrates visual data with somatosensory data from stretchable sensors. *Nature Electron*. 2020;3(9):563. (c) Zhou ZH, Chen K, Li XS, et al. Sign-to-speech translation using machine-learning-assisted stretchable sensor arrays. *Nature Electron*. 2020;3(9):571. (d) Wu R, Seo S, Ma L, Bae J, Kim T. Full-fiber auxetic-interlaced yarn sensor for sign-language translation glove assisted by artificial neural network. *Nano-Micro Lett*. 2022;14(1):139. (e) Hou C, Tai G, Liu Y, Wu Z, Liang X, Liu X. Borophene-based materials for energy, sensors and information storage applications. *Nano Res Energy*. 2023;2(2):e9120051. (f) Xu F, Jin X, Lan C, et al. 3D arch-structured and machine-knitted triboelectric fabrics as self-powered strain sensors of smart textiles. *Nano Energy*. 2023;109:108312. (g) Sheng F, Zhang B, Cheng R, et al. Wearable energy harvesting-storage hybrid textiles as on-body self-charging power systems. *Nano Res Energy*. 2023;2(4):e9120079. (h) Zhang R, Lin J, He T, et al. High-performance piezoresistive sensors based on transfer-free large-area $PdSe_2$ films for human motion and health care monitoring. *InfoMat*. 2023;6:e12484.
9. (a) Amjadi M, Kyung K-U, Park I, Sitti M. Stretchable, skin-mountable, and wearable strain sensors and their potential applications: a review. *Adv Funct Mater*. 2016;26(11):1678. (b) Cheng Y, Wang RR, Sun J, Gao L. A stretchable and highly sensitive graphene-based fiber for sensing tensile strain, bending, and torsion. *Adv Mater*. 2015;27(45):7365. (c) Wu R, Ma L, Patil A, et al. All-textile electronic skin enabled by highly elastic spacer fabric and conductive fibers. *ACS Appl Mater Interfaces*. 2019;11(36):33336. (d) Zhou Q, Pan J, Deng S, Xia F, Kim T. Triboelectric nanogenerator-based sensor systems for chemical or biological detection. *Adv Mater*. 2021;33(35):2008276. (e) Feng ZP, Hao YN, Qin J, et al. Ultrasmall barium titanate nanoparticles modulated stretchable dielectric elastomer sensors with large deformability and high sensitivity. *InfoMat*. 2023;5:e12413.
10. (a) Cao X, Ye C, Cao L, Shan Y, Ren J, Ling S. Biomimetic spun silk ionotronic fibers for intelligent discrimination of motions and tactile stimuli. *Adv Mater*. 2023;35(36):2300447. (b) Ye C, Dong S, Ren J, Ling S. Ultrastable and high-performance silk energy harvesting textiles. *Nano-Micro Lett*. 2020;12:1.
11. Wu R, Liu S, Lin Z, Zhu S, Ma L, Wang ZL. Industrial fabrication of 3D braided stretchable hierarchical interlocked fancy-yarn triboelectric nanogenerator for self-powered smart fitness system. *Adv Energy Mater*. 2022;12(31):2201288.
12. (a) Pan J, Hao B, Song W, et al. Highly sensitive and durable wearable strain sensors from a core-sheath nanocomposite yarn. *Compos B: Eng*. 2020;183:107683. (b) Alam MM, Crispin X. The past, present, and future of piezoelectric fluoropolymers: towards efficient and robust wearable nanogenerators. *Nano Res Energy*. 2023;2(4):107683.
13. (a) Zhang MC, Wang CY, Wang Q, Jian MQ, Zhang YY. Sheath-core graphite/silk fiber made by dry-meyer-rod-coating for wearable strain sensors. *ACS Appl Mater Inter*. 2016;8(32):20894. (b) Ma L, Wu R, Liu S, et al. A machine-fabricated 3D honeycomb-structured flame-retardant triboelectric fabric for fire escape and rescue. *Adv Mater*. 2020;32(28):2003897.
14. Wu R, Ma L, Liu S, et al. Fibrous inductance strain sensors for passive inductance textile sensing. *Mater Today Phys*. 2020;15:100243.
15. (a) Zhang Z, He T, Zhu M, et al. Deep learning-enabled triboelectric smart socks for IoT-based gait analysis and VR applications. *npj Flex Electron*. 2020;4(1):1. (b) Zhu M, Sun Z, Zhang Z, et al. Haptic-feedback smart glove as a creative human-machine interface (HMI) for virtual/augmented reality applications. *Sci Adv*. 2020;6(19):eaaz8693.
16. (a) Zhang HJ, Han WQ, Xu K, et al. Stretchable and ultrasensitive intelligent sensors for wireless human-machine manipulation. *Adv Funct Mater*. 2021;31(15):2009466.
17. (a) Chen S, Liu H, Liu S, et al. Transparent and waterproof ionic liquid-based fibers for highly durable multifunctional sensors and strain-insensitive stretchable conductors. *ACS Appl Mater Interfaces*. 2018;10(4):4305. (b) Wang Y, Hao J, Huang Z, et al. Flexible electrically resistive-type strain sensors based on reduced graphene oxide-decorated electrospun polymer fibrous mats for human motion monitoring. *Carbon*. 2018;126:360. (c) Wu J, Wang Z, Liu W, Wang L, Xu F. Bioinspired superelastic electroconductive fiber for wearable electronics. *ACS Appl Mater Interfaces*. 2019;11(47):44735. (d) Duan Z,

Jiang Y, Wang S, et al. Inspiration from daily goods: a low-cost, facilely fabricated, and environment-friendly strain sensor based on common carbon ink and elastic core-spun yarn. *ACS Sustain Chem Eng*. 2019;7(20):17474. (e) Wang L, Tian M, Zhang Y, et al. Helical core-sheath elastic yarn-based dual strain/humidity sensors with MXene sensing layer. *J Mater Sci*. 2020;55:6187. (f) Li W, Xu F, Liu W, et al. Flexible strain sensor based on aerogel-spun carbon nanotube yarn with a core-sheath structure. *Compos Part A Appl Sci Manuf*. 2018;108:107. (g) Wang Z, Huang Y, Sun J, et al. Flexible strain sensor based on aerogel-spun carbon nanotube yarn with a core-sheath structure. *ACS Appl Mater Interfaces*. 2016;8(37):24837. (h) Li X, Hua T, Xu B. Electromechanical properties of a yarn strain sensor with graphene-sheath/polyurethane-core. *Carbon*. 2017;118:686. (i) Li L, Shi P, Hua L, et al. Design of a wearable and shape-memory fibriform sensor for the detection of multi-modal deformation. *Nanoscale*. 2018;10(1):118. (j) Wu J, Ma Z, Hao Z, et al. Sheath–core fiber strain sensors driven by in-situ crack and elastic effects in graphite nanoplate composites. *ACS Appl Nano Mater*. 2019;2:(2)750. (k) Tang Z, Jia S, Wang F, et al. Highly stretchable core–sheath fibers via wet-spinning for wearable strain sensors. *ACS Appl Mater Interfaces*. 2018;10(7):6624. (l) Park JJ, Hyun WJ, Mun SC, Park YT, Park OO. Highly stretchable and wearable graphene strain sensors with controllable sensitivity for human motion monitoring. *ACS Appl Mater Interfaces*. 2015;7(11):6317. (m) Wang X, Qiu Y, Cao W, Hu P. Highly stretchable and conductive core–sheath chemical vapor deposition graphene fibers and their applications in safe strain sensors. *Chem Mater*. 2015;27(20):6969. (n) Zeng Z, Hao B, Li D, Cheng D, Cai G, Wang X. Large-scale production of weavable, dyeable and durable spandex/CNT/cotton core-sheath yarn for wearable strain sensors. *Compos Part A Appl Sci Manuf*. 2021;149:106520.

18. Loper M, Mahmood N, Romero J, Pons-Moll G, Black MJ. SMPL: a skinned multi-person linear model. *ACM Trans Graph*. 2015;34(6):1-16.
19. ISO 20685-1:2018. 3-D scanning methodologies for internationally compatible anthropometric databases. Accessed February 22, 2024. https://www.iso.org/standard/63260.html.
20. Long M, Cao Y, Wang J, Jordan M. Learning transferable features with deep adaptation networks. Presented at *Michael Jordan Proceedings of the 32nd International Conference on Machine Learning*, Lille, France. 2015;37:97-105.
21. Cao Z, Hidalgo Martinez G, Simon T, Wei S-E, Sheikh YA. OpenPose: Realtime multi-person 2D pose estimation using part affinity fields. *IEEE Trans Pattern Anal Mach Intell*. 2019;43(1):172-186.

SUPPORTING INFORMATION

Additional supporting information can be found online in the Supporting Information section at the end of this article.

How to cite this article: Wu R, Ma L, Chen Z, et al. Stretchable spring-sheathed yarn sensor for 3D dynamic body reconstruction assisted by transfer learning. *InfoMat*. 2024;e12527. doi:10.1002/inf2.12527